Letters

A Novel Multi-Scale Frequency Regulation Method of Hybrid Rectifier and Its Specific Application in Electrolytic Hydrogen Production

Xin Meng, *Member, IEEE*, Luling Jiang, Mingzhi He, *Member, IEEE*, Xueqing Wang, *Member, IEEE*, and Jinjun Liu, *Fellow, IEEE*

***Abstract*—Due to the limitation of existing rectifier, it is difficult to realize the multiscale frequency regulation (FR) of rectifier interfaced large-size (multi MW scale) load. To overcome this issue, a novel coordinative control method of hybrid rectifier is proposed to realize multiscale FR, and it is specifically applied in electrolytic hydrogen production (EHP) load. The auxiliary converter in hybrid rectifier is utilized to realize short-time/low-power/small-energy scale FR, such as inertia support during transient state, smoothing the rate of change of frequency and buying time for the action of silicon controlled rectifier (SCR). SCR in hybrid rectifier takes the responsibility of FR of long-time/high-power/large-energy scale, such as primary or secondary FR. The operation characteristic of large-size EHP load is reconstructed so that it obtains the multiscale FR capability. The effectiveness of proposed method is verified by experimental results.**

***Index Terms*—Electrolytic hydrogen production (EHP), hybrid rectifier, inertia support, multiscale frequency regulation (FR).**

I. Introduction

With the increasing penetration of power electronic equipment in electrical power system (EPS), as shown in Fig. 1, it is better for both the inverter-interfaced renewable energy source (or batteries) and the rectifier-interfaced adjustable loads (as if electrolytic stack) to possess the multiscale frequency regulation (FR) capability such as inertia support (time scale of millisecond), primary FR (time scale of several seconds) and secondary FR (time scale of tens of seconds) to maintain the system frequency stability [1]. Various virtual synchronous generator and droop control methods have been proposed for inverters to realize FR [2], [3]. In addition, lots of studies are conducted to achieve the FR of rectifier-interfaced adjustable loads. The rectifiers can be divided into two kinds according to switching frequency: pulsewidth modulation (PWM) rectifier and silicon controlled rectifier (SCR).

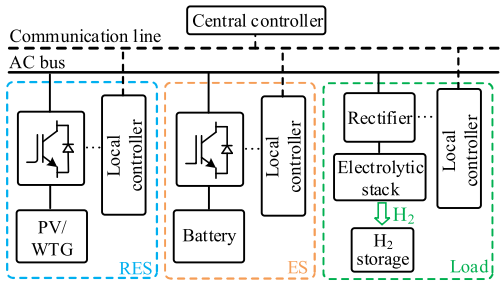

Fig. 1. Typical structure of EPS with large penetration of power electronic equipment.

SCR has high power level, low cost, but poor dynamic performance; thus, it is usually used to realize the primary and secondary FR. For example, the author studied the viability of integration of demand side response of large scale electrolyzer facilities into electrical ancillary services markets [4]. The control strategy of aluminum smelter loads to provide primary frequency support based on SCR and self-saturable reactor was proposed in [5]. In [6], the power-to-gas plant's ability to take part in the frequency containment control market was considered, and the primary FR behavior of a 9 MW SCR-interfaced electrolyzer under different power up ramp rates was studied. Whereas, it is difficult for SCR-interfaced load to achieve inertia support due to its slow response speed (the control period of SCR is 20 ms for grid frequency of 50 Hz, and 16.7 ms for grid frequency of 60 Hz).

In reverse, because the PWM rectifier has fast dynamic performance and flexible controllability, the multiscale FR of PWM rectifier interfaced load can be realized. For example, the virtual synchronous machine (VSM) control was adopted in PWM rectifier of variable frequency air conditioner to participate in rapid FR [7], and the secondary FR method of group of variable frequency air conditioner was also studied. The control structure of PWM rectifier for electrolyzer was divided into fast and slow loops in [8], the fast loop is responsible for responding to sudden events, such as voltage and frequency mutation, and the slow one focuses on economic optimization and frequency restoration.

Manuscript received 8 July 2022; revised 3 September 2022; accepted 14 September 2022. Date of publication 19 September 2022; date of current version 10 October 2022. This work was supported by National Natural Science Foundation of China under Grant 52207217 and the Fundamental Research Funds for the Central Universities. *(Corresponding author: Xueqing Wang.)*

Xin Meng, Luling Jiang, Mingzhi He, and Xueqing Wang are with the Electrical Engineering School of Sichuan University, Chengdu 610065, China (e-mail: mengxin_pe@163.com; 597691868@qq.com; darmyhe@vip.126.com; wangxueqing231@163.com).

Jinjun Liu is with the State Key Lab of Electrical Insulation and Power Equipment, School of Electrical Engineering, Xi'an Jiaotong University, Xi'an 710049, China (e-mail: jjliu@xjtu.edu.cn).

Color versions of one or more figures in this article are available at https://doi.org/10.1109/TPEL.2022.3207601.

Digital Object Identifier 10.1109/TPEL.2022.3207601

The author proposed a control method that allows PWM rectifier interfaced electric vehicle charger to effectively respond to grid frequency fluctuations and add high virtual inertia by online regulating the charging level in [9]. However, due to the low power level and high cost of PWM rectifier, they are mainly used in small-size (several kW to hundreds of kW scale) load. It is uneconomical and unreliable to adopt PWM rectifier to perform FR in large-size (multi MW scale) loads.

The hybrid rectifier consists of SCR and PWM converter in parallel, and it is economically suitable for large-size load, in which the SCR undertakes the main load power and the PWM converter is utilized to compensate the ac side harmonics and dc side ripples of SCR [10], [11]. The SCR and PWM converter in hybrid rectifier have different power levels and dynamic performances, thus, it is suitable to realize multiscale FR. However, as far as the author known, there is seldom research about the multiscale FR method of hybrid rectifier.

This letter studies the feasibility and implementation method of multiscale FR of hybrid rectifier for large-size (multi MW scale) load. The electrolytic stack has large capacity, flexible consuming power and fast response speed [12], which is a natural physical resource that can provide FR energy; thus, the proposed multiscale FR method of hybrid rectifier is specifically applied in electrolytic hydrogen production (EHP). A coordinative control method of different converters in hybrid rectifier is put forward to effectively control the response characteristic of EHP load. The PWM converter in hybrid rectifier can provide inertia support, smoothing the rate of change of frequency (ROCOF) and buying time for the action of SCR, and the SCR acts as FR main force and realizes the primary FR by regulating its firing angle. Then, the qualitative and quantitative comparison of feasibility of different rectifiers is presented. Finally, a laboratory-scale experiment based on hybrid rectifier and electrolyzer is conducted to verify the effectiveness of proposed method.

II. Multiscale FR Method of Hybrid Rectifier

The main circuit and control block of hybrid rectifier with multiscale FR capability is shown in Fig. 2.

The hybrid rectifier adopts the topology the author proposed before [11], consists of a six-pulse SCR and an auxiliary converter, including a PWM voltage source converter (VSC) and a phase-shift-full-bridge (PSFB) converter. When the power imbalance leads to frequency variation, taking the frequency dropping as an example, the hybrid rectifier should decrease the EHP power, which equals to output active power to ac bus, and the equivalent output power is shown in Fig. 3.

First, the auxiliary converter rapidly adjusts the power flowing through itself to realize the short-time/low-power/ small-energy scale frequency support and slow down the rate of descent of frequency. Second, the SCR acts as the main force of FR and adjusts the hydrogen production power to achieve primary FR and even secondary FR (in this article, the secondary FR is not considered). Then the auxiliary converter gradually decreases its equivalent output power for FR, and the power flowing through auxiliary converter and SCR in steady state depends on their droop coefficients, respectively.

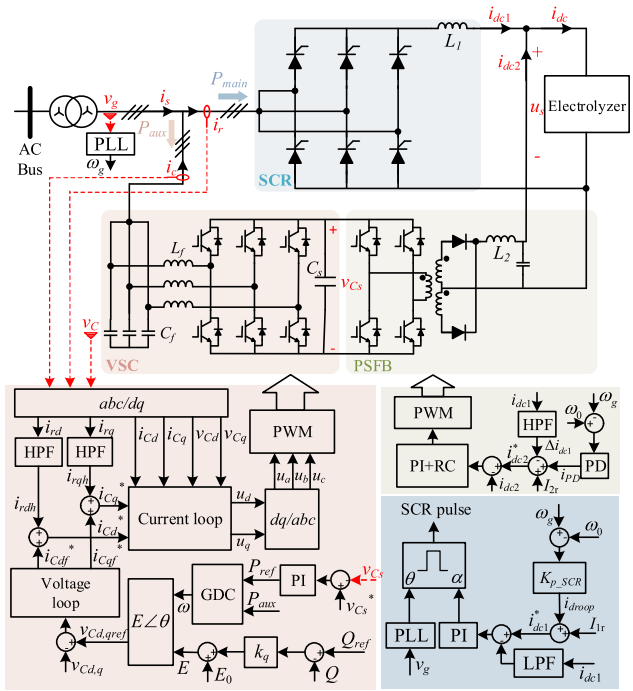

Fig. 2. Main circuit and control block of proposed hybrid rectifier with multiscale FR capability.

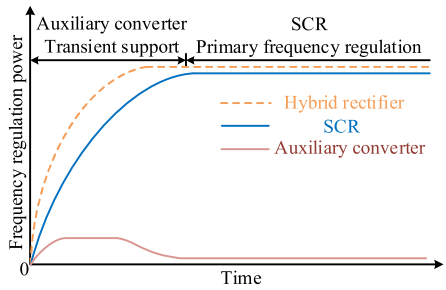

Fig. 3. Schematic diagram of equivalent output active power of hybrid rectifier for FR.

1) *Control of VSC:* The VSC operates with generalized droop control (GDC), and the control equation of active power loop is given as follows, which can provide inertia and damping during transient state

$$\omega = \omega_0 + k_p \cdot \frac{\tau_1 s + 1}{(T_1 s + 1)(T_2 s + 1)} \cdot (P_{\text{ref}} - P_{\text{aux}}) \quad (1)$$

where ω_0 is the nominal angular frequency, k_p is droop coefficient, τ_1, T_1, and T_2 are different time constants of lead or lag units, P_{ref} is the active power reference produced by the control of dc bus voltage v_{Cs} as listed

$$P_{\text{ref}} = \left(k_{p\_\text{DC}} + \frac{k_{i\_\text{DC}}}{s} + k_{d\_DC} s\right)(v_{Cs}^{*} - v_{Cs}). \quad (2)$$

Through regulation of v_{Cs}, the input active power of VSC equals the output active power of PSFB converter in steady state. The VSM control can also be used in VSC, the GDC is selected herein because it has better power tracking performance.

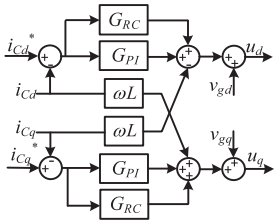

Fig. 4. Control block of current loop of VSC.

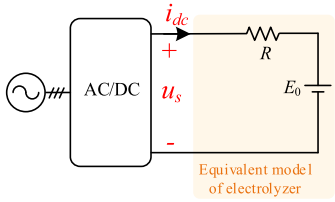

Fig. 5. Simplified equivalent model of electrolyzer.

Namely, compared with VSM control, the GDC can suppress oscillation and reduce settling time of active power P when the power reference P_{ref} changes [13]. According to (2), the VSC with GDC has better dc-bus voltage regulation performance than that with VSM control.

The outputs of active power control loop and reactive power control loop constitute the voltage reference $v_{Cd,q\text{ref}}$, and through the control of voltage loop, the fundamental current reference $i_{Cd,qf}{}^*$ are produced, as shown in Fig. 2.

The harmonics $i_{rd,qh}$ of SCR current are extracted by the high pass filter. The d-axis current reference of VSC $i_{Cd}{}^*$ is consisted of $i_{Cdf}{}^*$ and i_{rdh}, as for q-axis, and there are

$$\begin{cases} i_{Cd}^* = i_{Cdf}^* + i_{rdh} \\ i_{Cq}^* = i_{Cqf}^* + i_{rqh} \end{cases}. \tag{3}$$

Both the proportional and integral (PI) controller G_{PI} and repetitive controller (RC) G_{RC} are used in the current loop to ensure that the d- and q-axes grid current of VSC $i_{Cd,q}$ can follow their references $i_{Cd,q}{}^*$, as illustrated in Fig. 4.

2) *Control of PSFB converter:* As shown in Fig. 2, a current control loop is adopted, and the current reference i_{dc2}^* includes three parts: Δi_{dc1}, i_{PD}, and $I_{2\text{r}}$, as given in,

$$i_{\text{dc2}}^* = I_{2r} + i_{\text{PD}} - \Delta i_{dc1} \tag{4}$$

where $I_{2\text{r}}$ is the dc offset value, $\Delta i_{\text{dc1}}$is the ripple of dc current of SCR, and i_{PD} is the output of proportion and derivative (PD) controller, which regulates the output active power of PSFB converter according to the system frequency and maintains the power balance inside the auxiliary converter. Without i_{PD}, the output active power of PSFB converter is fixed, then for the control of VSC, it is contradictory to regulate dc-bus voltage v_{Cs} constant and to change input active power to participate in short-time scale FR. The structure of parallel PI regulator and RC is utilized in the current loop of PSFB converter to make sure that the power regulation and ripple compensation can be realized simultaneously.

3) *Control of SCR:* A closed loop of dc output current of SCR is adopted to regulate the firing angle α to guarantee that the dc component of i_{dc1} can follow its reference i_{dc1}^*, which consists of $I_{1\text{r}}$ and i_{droop}, as shown

$$i_{\text{dc1}}^* = I_{1r} + K_{p\_\text{SCR}} \cdot (\omega_g - \omega_0). \tag{5}$$

$I_{1\text{r}}$ decides the main hydrogen production power flowing through SCR, which can be regulated according to the upper level controller to take part in the secondary even tertiary FR, and it is not considered in this article; a positive feedback relationship between ω_g and $i_{\text{dc1}}{}^*$ is built to realize the primary FR of SCR. For example, when the system frequency ω_g drops, which indicates the generating power deficient, and $i_{\text{dc1}}{}^*$ falls with ω_g to decrease the hydrogen production power to maintain the system power balance.

4) *Quantified analysis of capacity proportion of converters and design of control parameters in hybrid rectifier:* From the perspective of compensation of dc-side ripples, ac -side harmonics and reactive power of SCR, the capacity of VSC, PSFB converter, and SCR are 400 kVA, 100 kVA, and 1 MVA, respectively, for a 1 MVA hybrid rectifier, and the reason was given in [11]. Herein, the analysis of capacity proportion of converters will be conducted from viewpoint of FR power and energy.

First, the capacity selection and control parameter design of SCR are presented. The operating range of proton exchange membrane (PEM) electrolyzer is 20%–120% of its rated power [14]. It is assumed that the steady-state operating point of electrolyzer is 70% rated power in this article, and the bidirectional adjustable power range is exactly 50%; thus, the power range of 500 kW can be used for FR for a 1 MW electrolyzer. SCR has certain overload ability, and a 1 MVA SCR is sufficient for a 1 MW electrolyzer even if the electrolyzer at 120% operating point.

The simplified equivalent model of electrolyzer is shown in Fig. 5, the terminal voltage of electrolyzer (u_s) is equal to the sum of stack reverse voltage of electrolyzer (E_0) and the voltage drop across all ohmic elements of the electrolyzer, for example, busbar, cathode and anode blocks, electrolyte [15].

The stack reverse voltage (E_0) accounts for nearly 60% of rated terminal voltage of electrolyzer [16], namely, for a 1 MW electrolyzer with rated terminal voltage (u_s) of 200 V and current (i_{dc}) of 5000 A, its stack reverse voltage is nearly 120 V; thus, the *V–I* relation is listed as (6) and the *V–I* curve of electrolyzer is shown in Fig. 6. The 20% rated power (equaling 200 kW) corresponds to the dc current of 1404 A, and the 120% rated power (equaling 1.2 MW) corresponds to the dc current of 5687 A

$$u_s = R \cdot i_{\text{dc}} + E_0 = 0.016 \cdot i_{\text{dc}} + 120. \tag{6}$$

According to [17], the droop coefficient m in active power (P)—angular frequency (ω) droop control is designed as (7),

$$m = \delta\omega / \delta P_{\max} \tag{7}$$

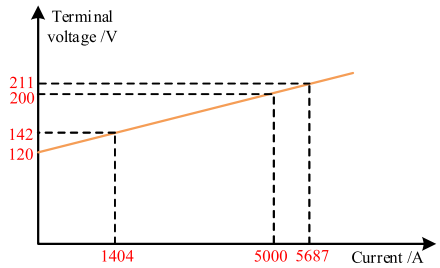

Fig. 6. *V—I* curve of electrolyzer.

where $\delta\omega$ is the maximum allowed angular frequency deviation and $\delta P_{\max}$ is the maximum adjustable active power range. Therefore, the droop coefficient K_{p_SCR} of SCR in (5) between dc output current and angular frequency can be analogously calculated as

$$K_{p\_\mathrm{SCR}} = \delta I/\delta\omega = \frac{5687-1404}{2\pi\cdot(50.5-49.5)} = 682. \tag{8}$$

Second, the relationship among capacity of auxiliary converter, control parameter, and inertia and damping support ability is analyzed. According to [13], the inertia and damping of GDC and VSM control can be approximately equal by selecting proper control parameters in GDC, and because the order of VSM model is lower than GDC model, the former one is used to simplify analysis.

Without considering primary FR function, the swing equation of VSM and power angle are listed as (9), in which -P_{aux} is used to follow the inverter direction, and the transmitted active power from ac bus to auxiliary converter is calculated as (10) when neglecting the loss of transformer

$$\begin{cases} P_{\mathrm{ref}} - (-P_{\mathrm{aux}}) - D\cdot(\omega-\omega_g) = J\omega_0\frac{d\omega}{dt} \\ \delta = \frac{\omega-\omega_g}{s} \end{cases} \tag{9}$$

$$P_{\mathrm{aux}} = \frac{V_C V_g \delta}{X} \tag{10}$$

where D is damping coefficient, J is the moment of inertia, ω_0 is nominal angular frequency, δ is power angle, ω_g is angular frequency of secondary side voltage of transformer (v_g in Fig. 2), V_g is the amplitude of v_g, V_C is the amplitude of capacitor voltage of VSC, and X is the inductive reactance of transformer and line impedance. The small signal transfer function from $\Delta\omega_g$ to ΔP_{aux} can be calculated as (11) combining (9) and (10). When there is a step change of system frequency $\Delta\omega_g$, ΔP_{aux} is represented as (12)

$$\frac{\Delta P_{\mathrm{aux}}}{\Delta\omega_g} = \frac{V_C V_g J\omega_0 s}{J\omega_0 X s^2 + DXs + V_C V_g} \tag{11}$$

$$\Delta P_{\mathrm{aux}} = \frac{V_C V_g J\omega_0 s}{J\omega_0 X s^2 + DXs + V_C V_g}\cdot\frac{\Delta\omega_g}{s}. \tag{12}$$

The step response of $\Delta P_{\mathrm{aux}}/\Delta\omega_g$ is shown in Fig. 7, where V_C = 121 V, V_g = 121 V (the dc output voltage of SCR is assumed as 200 V, thus, the RMS value of v_g is 85.5 V, and V_g = 121 V), X = 1.256 Ω, D = $5\cdot10^4$, and J = 203 kg·m^2 (the inertia constant H = $0.5J\omega^2/S_n$, in which S_n is the rated capacity of hybrid rectifier

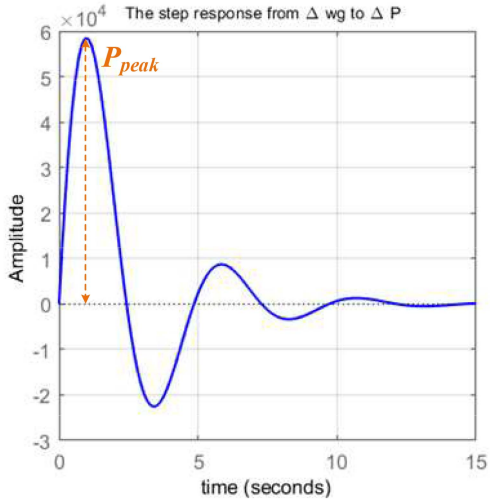

Fig. 7. Step response of transfer function $\Delta P_{\mathrm{aux}}/\Delta\omega_g$.

and equals 1 MVA, and typical H is around 2–10 s [18]; thus, J = 203 kg·m^2 for H = 10 s). To make sure the converter with GDC has similar inertia and damping characteristics, the time constant τ_1, T_1, and T_2 can be designed according to [13].

As shown in Fig. 7, it is clear that the smallest adjustable power range of auxiliary converter to realize inertia and damping support is determined by the peak value P_{peak}, namely, at least 60 kVA capacity should be reserved for auxiliary converter. If the control parameters J and D, or the main circuit parameters V_C, V_g and X change, the peak value in Fig. 7 will change and so on the reserved capacity of auxiliary converter.

Because the PSFB converter in auxiliary converter can only transmit power in single direction, its capacity increases from 100 kVA in [13] to 200 kVA to ensure that the auxiliary converter has an adjustable power range of 100 kW for FR no matter frequency rises or falls. The capacity of VSC is designed as 400 kVA in [13] to compensate the reactive power of SCR, and it is enough to transmit the 100 kW active power for FR but sacrificing a certain degree of reactive power compensation ability during FR process. Except for 60 kW used to provide inertia and damping support, there is still 40 kW active power for primary FR; thus, the droop coefficient can be designed as $1.57\cdot10^{-4}$ according to (7).

The FR energy during the transient process can be integrated from the ΔP_{aux} in (12), as shown in Fig. 8, and it is much less than the FR energy transmitted through SCR.

III. Comparison of SCR, PWM Rectifier and Hybrid Rectifier

Different kinds of rectifiers including SCR, PWM rectifier, and hybrid rectifier can be utilized for EHP, and they will be compared from three aspects: the feasibility of multiscale FR; the cost of same power level rectifier; and the reliability.

First, the feasibility of multiscale FR of EHP load based on different rectifiers is compared. Due to the poor dynamic

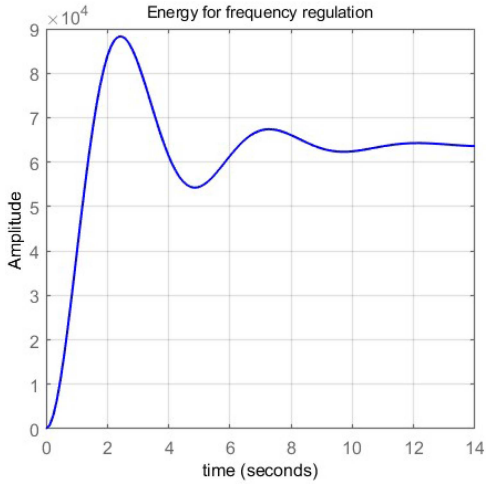

Fig. 8. FR energy for inertia and damping support during transient process.

TABLE I
COST OF DIFFERENT RECTIFIERS

Topology (1 MVA)	T1	T2	T3
Transformer	$ 20,000	$ 20,000	$ 20,800
Capacitor and inductor	$ 1,100	$ 5,950	$ 4,480
Power switching device	$ 3,600	$ 16,500	$ 11,800
Control, sensor, and drive circuit	$ 1,500	$ 5,000	$ 5,100
Total	$ 26,200	$ 47,450	$ 42,180

T1: 6 pulse SCR T2: PWM rectifier
T3: Hybrid rectifier (200 kVA PSFB, 400 kVA VSC and 1 MVA SCR)

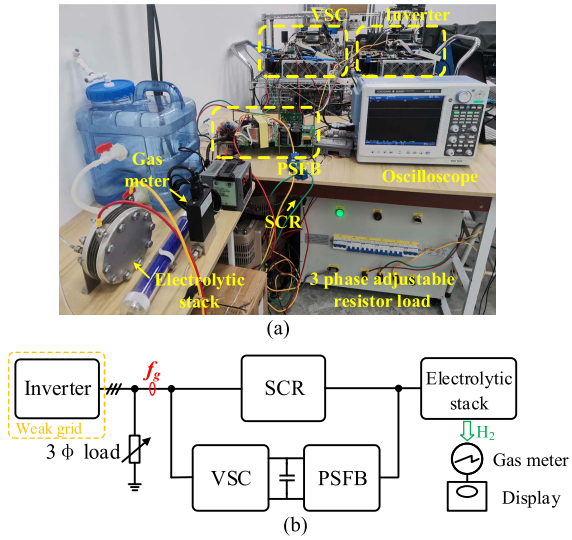

Fig. 9. Experimental platform. (a) Photograph (b) Diagram block.

TABLE II
EXPERIMENTAL PARAMETERS

Parameter	Value	Parameter	Value
ac bus voltage	63 V	rated frequency	50 Hz
dc bus voltage v_{Cs}	130 V	dc voltage (mean)	55 V
SCR capacity	50 kVA	VSC capacity	10 kVA
PSFB capacity	5 kVA		

performance of SCR, it cannot realize the short-time/low-power/small-energy scale FR. In reverse, the PWM rectifier has fast dynamic performance and flexible controllability, and it can realize multiscale FR but with high cost; thus, it is mainly used for short-time/low-power/small-energy scale FR in most cases. Whereas, the hybrid rectifier can realize multiscale FR economically through the coordination of different converters.

Second, the cost comparison of different MVA level rectifiers is given in Table I, which is based on a particular estimation example and it can just be taken as an approximation. The cost advantage of hybrid rectifier compared with PWM rectifier is further expanded with increase of rectifier capacity.

Third, the reliability of these rectifiers are compared. In engineering application, it is generally considered that the failure rate of power devices is constant, and the reliability of different power devices can be compared according to rule: low failure rate corresponding to high reliability of power devices. The base failure rate of thyristor is 22 FIT [19]; while the base failure rate of insulated gate bipolar translator (IGBT) module is estimated to be 100 FIT in the literature [20]. Thus, the thyristor is considered to be more reliable than IGBT under the same working conditions. SCR has highest reliability, and the reliability of PWM rectifier is lowest. If the full function of hybrid rectifier is considered, its reliability is lower than that of SCR, but even if the auxiliary converter of it breaks down, the hybrid rectifier can also operate as a common SCR, only the power quality is not as usual and the multiscale FR capability is loss.

Above all, the hybrid rectifier is feasible compared with SCR and PWM rectifier considering the multiscale FR capability, cost, and reliability.

IV. EXPERIMENTAL RESULTS

To verify the effectiveness of proposed multiscale FR method of hybrid rectifier, the experiment is conducted based on a low power experiment platform including an inverter, a hybrid rectifier, a PEM electrolyzer and an adjustable load, as shown in Fig. 9, and the experimental parameters are given in Table II. Due to the limited capacity of existing converters in our laboratory, their capacity ratio is not exactly consistent with the theoretical design mentioned earlier.

The inverter with droop control is used to mimic a weak grid; otherwise, if the hybrid rectifier and load connect with utility directly, when the load changes, the variation of load power will be undertaken by utility, and it cannot reflect the FR capability of hybrid rectifier. Because the supply voltage of electrolytic stack in our laboratory cannot exceed 9 V, and its equivalent resistance is 0.25 Ω and quite small. A resistor of 5 Ω is connected with electrolytic stack in series to divide voltage. The high precision gas meter is used to measure H_2 production rate.

The three-phase resistor load connecting at ac bus increases at instant t_1 and the system frequency drops. When the hybrid rectifier operates with proposed control method, the system frequency changes smoothly, as shown in Fig. 10, and the ROCOF is 0.314 rad/s, which means the EHP load with hybrid rectifier can provide virtual inertia. In addition, as given in Table III,

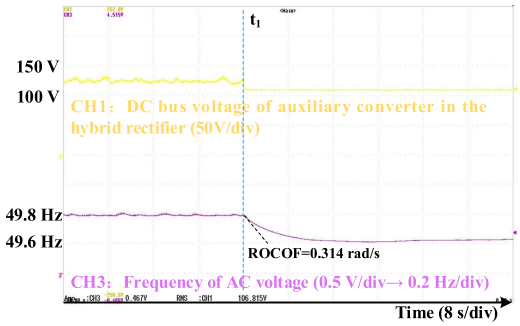

Fig. 10. Experimental results of hybrid rectifier in which VSC operates with GDC.

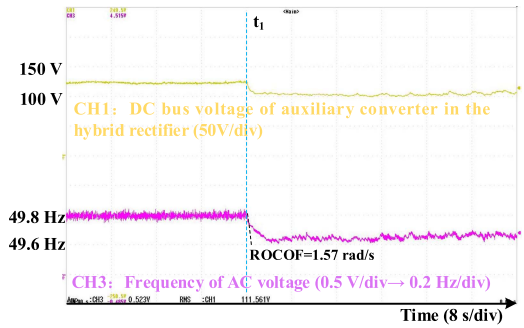

Fig. 12. Experimental results of hybrid rectifier in which VSC operates with droop control.

TABLE III
HYDROGEN PRODUCTION RATE

	Before load increase	After load increase
VSC with Droop control	124.2 mL/min	114.2 mL/min
VSC with GDC	126.9 mL/min	116.7 mL/min

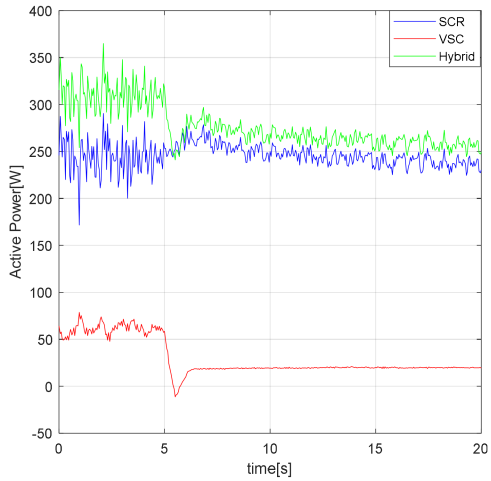

Fig. 11. EHP power flowing through SCR, VSC and hybrid rectifier when the VSC operates with GDC.

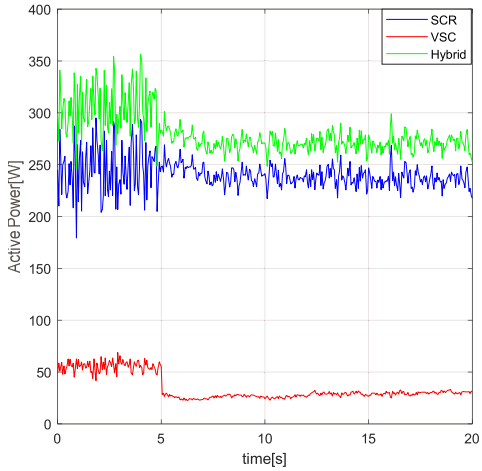

Fig. 13. EHP power flowing through SCR, VSC and hybrid rectifier when the VSC operates with traditional droop control.

before load increasing, the hydrogen production rate is 126.9 mL/min, and after load increasing, the hydrogen production rate decreases to 116.7 mL/min, which represents the hybrid rectifier decreases its hydrogen production power to realize the primary FR.

The active power flowing through SCR, VSC and hybrid rectifier are measured by HIOKI power analyzer 6001, updated and recorded per 50 ms. When the load increases at 5 s, the EHP power flowing through VSC decreases largely to provide virtual inertia, then it returns back a few to realize primary FR, as the red line in Fig. 11 shows. The power flowing through SCR decreases slowly (blue line in Fig. 11) to another constant value to realize primary FR. Above all, the total power flowing through hybrid rectifier (green line in Fig. 11) decreases largely at first to provide virtual inertia during transient state and then returns to a constant value to realize primary FR.

When the VSC operates with traditional droop control, and SCR and PSFB converter still operate with proposed control method, it is easy to find that the frequency changes quickly (ROCOF = 1.57 rad/s), as shown in Fig. 12, which means the inertia is insufficient. The hydrogen production rate is about 124.2 and 114.2 mL/min, respectively, before and after load changing, as given in Table III, and the difference is also about 10 mL/min. The active power flowing through VSC, SCR and hybrid rectifier is shown in Fig. 13, no power is transmitted to ac bus to provide virtual inertia when the load changes, and only the primary FR is realized.

V. CONCLUSION

A novel multitime/multipower/multienergy scale FR method of hybrid rectifier is proposed and specifically applied in EHP. The auxiliary converter in hybrid rectifier can realize short-time/low-power/small-energy scale FR, such as inertia and damping support, smoothing the ROCOF and buying time for the action of SCR. Then SCR acts as main force of FR and realizes the primary even secondary FR by regulating its firing angle. The operation characteristic of EHP load is reconstructed by the coordination of converters in hybrid rectifier, obtaining the multiscale FR capability economically.

REFERENCES

[1] B. Guha, R. Jain, and S. Veda, "Bulk grid frequency support using electrolyzers," in *Proc. IEEE Ind. Appl. Soc. Annu. Meeting*, 2020, pp. 1–5.

[2] L. Xiong, L. Liu, X. Liu, and Y. Liu, "Frequency trajectory planning based strategy for improving frequency stability of droop-controlled inverter based standalone power systems," *IEEE J. Emerg. Sel. Topics Circuits Syst.*, vol. 11, no. 1, pp. 176–187, Mar. 2021.

[3] J. Liu, Y. Miura, H. Bevrani, and T. Ise, "Enhanced virtual synchronous generator control for parallel inverters in microgrids," *IEEE Trans. Smart Grid*, vol. 8, no. 5, pp. 2268–2277, Sep. 2017.

[4] S. V. García et al., "Integration of Power-to-Gas conversion into dutch electrical ancillary services markets," in *Proc. 12th Conf. Energy Econ. Technol.*, 2018, pp. 1–7.

[5] P. Bao, "Coordinated active power/frequency control from supply, work, and demand sides considering participation of aluminum smelter load," M.S. thesis, Shandong Univ., 2021.

[6] P. Pasi et al., "Frequency regulation possibilities of power-to-gas plants in grids including high shares of renewable energy production," in *Proc. 10th Int. Renew. Energy Storage*, 2016, pp. 1–11.

[7] D. Wang, "Research on regulation technology of inverter air conditioning load virtual synchronous machine for fast grid frequency modulation," M.S. thesis, SouthEast Univ., 2020.

[8] M. Mohanpurkar et al., "Electrolyzers enhancing flexibility in electric grids," *Energies*, vol. 10, no. 11, pp. 1–17, 2017.

[9] H. Jafari, M. Moghaddami, T. O. Olowu, A. I. Sarwat, and M. Mahmoudi, "Virtual inertia-based multipower level controller for inductive electric vehicle charging systems," *IEEE J. Emerg. Sel. Topics Power Electron.*, vol. 9, no. 6, pp. 7369–7382, Dec. 2021.

[10] S. Bintz, M. Fischer, and J. Roth-Stielow, "Parallel rectifier for regenerative hydrogen production utilizing a combination of thyristor and PWM-based topologies," in *Proc. 20th Eur. Conf. Power Electron. Appl.*, 2018, pp. 1–10.

[11] X. Meng, M. Chen, M. He, X. Wang, and J. Liu, "A novel high power hybrid rectifier with low cost and high grid current quality for improved efficiency of electrolytic hydrogen production," *IEEE Trans. Power Electron.*, vol. 37, no. 4, pp. 3763–3768, Apr. 2022.

[12] B. L. H. Nguyen, M. Panwar, R. Hovsapian, K. Nagasawa, and T. V. Vu, "Power converter topologies for electrolyzer applications to enable electric grid services," in *Proc. 47th Annu. Conf. IEEE Ind. Electron. Soc.*, 2021, pp. 1–6.

[13] X. Meng, J. Liu, and Z. Liu, "A generalized droop control for grid-supporting inverter based on comparison between traditional droop control and virtual synchronous generator control," *IEEE Trans. Power Electron.*, vol. 34, no. 6, pp. 5416–5438, Jun. 2019.

[14] X. Peng et al., "Experimental and analytical study of a proton exchange membrane electrolyser integrated with thermal energy storage for performance enhancement," *Int. J. Photoenergy*, vol. 2022, pp. 1–9, 2022.

[15] R. A. Ufa et al., "Analysis of the influence of the current-voltage characteristics of the voltage rectifiers on the static characteristics of hydrogen electrolyzer load," *Int. J. Hydrogen Energy*, vol. 46: pp. 33670–33678, 2021.

[16] D. S. Falcao et al., "A review on PEM electrolyzer modelling: Guidelines for beginners," *J. Cleaner Prod.*, vol. 261, pp. 1–10, 2020.

[17] J. M. Guerrero, L. Hang, and J. Uceda, "Control of distributed uninterruptible power supply systems," *IEEE Trans. Ind. Electron.*, vol. 55, no. 8, pp. 2845–2859, Aug. 2008.

[18] J. Alipoor, Y. Miura, and T. Ise, "Power system stabilization using virtual synchronous generator with alternating moment of inertia," *IEEE J. Emerg. Sel. Topics Power Electron.*, vol. 3, no. 2, pp. 451–458, Jun. 2015.

[19] D. O. Defence, *Military Handbook- Reliability Predication of Electronic Equipment (MIL-HDBK-217E)*, 1991.

[20] P. Tu, S. Yang, and P. Wang, "Reliability- and Cost-Based redundancy design for modular multilevel converter," *IEEE Trans. Ind. Electron.*, vol. 66, no. 3, pp. 2333–2342, Mar. 2019.